PHYSICAL REVIEW B VOLUME 46, NUMBER 19 15 NOVEMBER 1992-I

Transport spectroscopy of a confined electron system under a gate tip

J. Weis, R. J. Haug, K. v. Klitzing, and K. Ploog*
Max-Planck-Institut für Festkörperforschung, Heisenbergstrasse 1, D-7000 Stuttgart 80, Federal Republic of Germany
(Received 21 May 1992)

Conductance resonances measured for split-gate structures around threshold are interpreted in terms of single-electron tunneling through a quantum dot beneath the tip of the gate finger. Measurements at different values of source-drain voltage allow the spectroscopy of excited states for a fixed number of electrons in the quantum dot. The measured magnetic-field dependence of the conductance resonances is consistent with a minimal number of seven electrons in the quantum dot.

Coulomb-blockade effects were recently studied in arrays of small metallic tunnel junctions and also in semiconductor systems where a quantum dot is defined by split-gate techniques.[1] The Coulomb-blockade theory, developed for metallic systems has been applied to dots with a large number of electrons, taking into account the discrete energy-level spectrum in the dot,[2–4] and was used in experiments with a few tens of electrons.[5]

We present here investigations of conductance resonances appearing in split-gate devices around threshold. We interpret them in terms of transport through a quantum dot with a small number of electrons localized beneath the tip of a gate finger.

The metallic split-gate structure was deposited on a GaAs-$Al_xGa_{1-x}As$ heterostructure with a two-dimensional electron gas (2D EG). The 2D EG has an electron density of 3.4×10^{15} m^{-2} and an electron mobility of 60 m^2/Vs at a temperature T of 4.2 K. The geometry of the split-gate structure is shown in inset of Fig. 1. The 2D EG and the gate are separated by 86 nm. For the measurements at temperatures below 1 K a fixed voltage V_{G2} is applied to gate 2, so that the 2D EG under and around this gate is depleted ($V_{G2} = -1$ V, threshold is at -0.26 V). While sweeping the voltage V_G of gate 1, the current through the device is measured with an ac lock-in technique (effective ac drain source voltage is 5 μV, ac frequency is 13.4 Hz). A dc bias voltage could be added to the ac voltage.

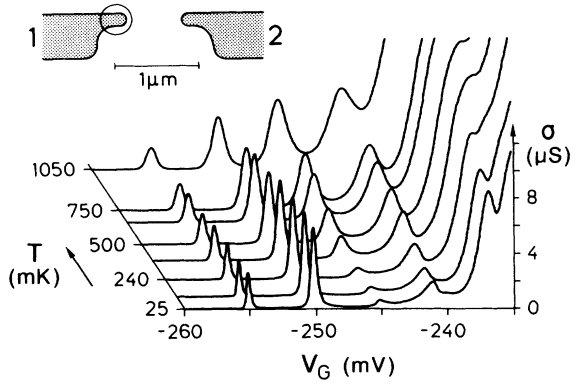

FIG. 1. Conductance σ vs gate voltage V_G for different temperatures T. Inset: Top view of the split-gate structure. The circle represents the region where we imagine the quantum dot.

Figure 1 shows a plot of conductance σ versus gate voltage V_G measured for different temperatures T. Around threshold we observe several sharp conductance resonances. Whereas the shape and amplitude of the conductance peaks are not affected by V_{G2}, the positions are shifted slightly by the same value for all peaks ($\Delta V_G/\Delta V_{G2} = 9 \times 10^{-4}$). Similar conductance resonances are seen for several samples. A warming-up and cooling-down process changes the conductance traces, but conductance resonances appear in all cases. Considering the insensitivity to the gate voltage V_{G2} and the vanishing of the conductance in between peaks, transport around threshold seems to take place through electronic states confined beneath the tip of the gate finger. This confined system is formed by spatial potential fluctuations which are caused by charged impurities possibly induced by the gate processing with electron-beam lithography. When increasing the voltage on gate 1 while keeping the voltage on gate 2 at a strong negative value, transport has to start at the tip of gate 1. The measurements, presented in the following, can consistently be interpreted in terms of transport through a quantum dot of the size of the tip of the gate, which has a diameter of 150 nm. The position of the dot is marked in the inset of Fig. 1 by a circle.

For transport through confined systems weakly coupled to the leads, Coulomb-blockade effects are expected. Gate voltage differences between conductance peaks are then given by the difference of the chemical potentials ξ for successive numbers of electrons in the confined system plus a Coulomb term e^2/C^3: $\Delta V_G = (\alpha e)^{-1}[\xi(N+1) - \xi(N) + e^2/C]$, where C describes the sum of the geometrical capacitances between the dot and the gates (C_G) and leads (C_l, C_r). $\alpha = C_G/C$ is the scaling factor between gate voltage and energy scale in the dot. The chemical potential ξ describes the change of total ground-state energy of interacting electrons when adding one electron in a confinement potential whose minimum is fixed at zero. For noninteracting electrons in the quantum dot $\xi(N)$ is equal to the single-electron eigenenergy E_N.[3,4]

Several remarkable features are seen in Fig. 1. Whereas at higher temperatures the peak shapes are symmetric

with gate voltage, as also observed in Ref. 5, they are not symmetric at the lowest temperatures. The full width at half maximum (FWHM) of the three lowest-lying conductance peaks increases linearly with temperature with the same slope for the temperature range given in Fig. 1. From this temperature dependence of the FWHM one gets the scaling factor α for the changes in V_G and the shift of the energy levels in the confined system related to the Fermi energy of the 2D EG reservoirs. As in Ref. 6 we assume a transmission resonance with Γ_0 the intrinsic FWHM between two fermion baths. To a first approximation the FWHM is then given by $(\alpha e)^{-1}(\Gamma_0+3.5k_BT)$ with k_B the Boltzmann constant and we obtain $\alpha = 0.5$ for our system. In Fig. 1 the amplitudes of the two lowest-lying peaks 1 and 2 are constant for the temperature increase between 25 mK and 0.3 K and decrease at higher temperatures. Conversely the amplitudes of peaks 3 and 4 increase for $T > 0.2$ K. A decrease in amplitude with increasing temperature is expected for well-separated energy levels in a quantum dot when the thermal broadening in the leads exceeds the intrinsic width of the resonance state.[3,7] An increase in amplitude can be explained by an adjacent state with a higher transmission through the barriers. By thermal overlap with this adjacent state the peak amplitude will rise and the conductance peak position in V_G will change, as observed for peaks 3 and 4 at higher temperatures. The apparent classification of peaks into pairs (1+2, 3+4) will be discussed later in more detail.

In the measurement of Fig. 1 the dc bias voltage V_{DS} was fixed at zero. Figure 2(a) shows the differential conductance $\delta I/\delta V_{DS}$ versus V_G at different V_{DS}. For increased dc bias the conductance peaks are broadened, and within the ranges of finite conductance additional peaks appear. In Fig. 2(b) the peak positions which correspond to steps in $I(V_{DS}, V_G)$ are plotted in the $V_{DS} - V_G$ plane. For comparison the peak positions observed for a magnetic field $B = 1$ T perpendicular to the 2D EG are also shown.

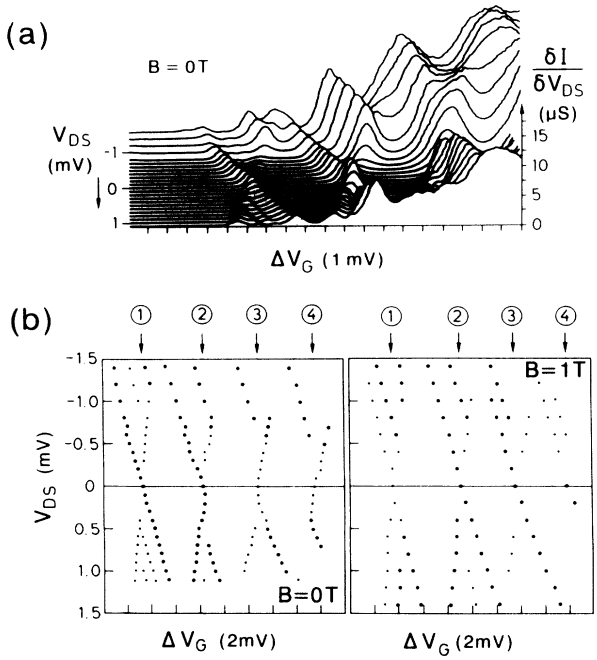

FIG. 2. (a) Differential conductance $\delta I/\delta V_{DS}$ vs gate voltage changes ΔV_G for different dc bias voltages V_{DS} ($B = 0$ T, $T = 730$ mK). (b) Positions of the maxima of the differential conductance in the V_{DS} vs ΔV_G plane for $B = 0$ T and $B = 1$ T. The peak indices are given above. Large dots correspond to large amplitudes.

In the following we discuss these observations in terms of single-electron tunneling.[4] During transport the number of electrons in the dot has to change from N to $(N + 1)$ and then from $(N + 1)$ to N (cotunneling[1] as a second-order effect is not considered here). The energy needed in adding the $(N + 1)$th electron to the dot is given by the chemical potential $\xi(N + 1)$ plus the electrostatic energy change $\Delta U(N + 1, V_G, V_{DS}) = e^2/2C + e(Ne - C_GV_G - C_rV_{DS})/C$ calculated for the circuit shown in Fig. 3(a) while V_G and V_{DS} are fixed. During tunneling through the barriers (from an occupied state in the emitter reservoir into the dot and from the dot into an empty state in the collector reservoir) the energy must to be conserved. So at $T = 0$ K transport may occur if

$$\mu_E \geq \xi(N+1) + \Delta U(N+1, V_G, V_{DS}) \geq \mu_C. \qquad (1)$$

μ_E (μ_C) is the electrochemical potential of the emitter (collector) reservoir. For positive (negative) V_{DS} in our circuit, as shown in Fig. 3(a), the electrochemical potentials are given by $\mu_E = \varepsilon_F + e|V_{DS}|$ ($\mu_E = \varepsilon_F$) and $\mu_C = \varepsilon_F$ ($\mu_C = \varepsilon_F - e|V_{DS}|$), where ε_F is the Fermi energy of the 2D EG in the reservoirs.

For nonzero dc bias V_{DS} the interval in which V_G satisfies Eq. (1) is broadened. The boundaries between transport and blockade in the $V_{DS} - V_G$ space are sketched in

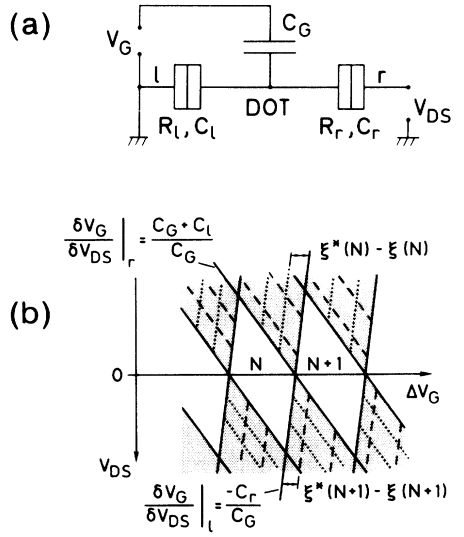

FIG. 3. (a) Schematic circuit used for the interpretation. (b) The different regions of conductance in the V_{DS} vs ΔV_G plane. The shaded regions representing transport surround regions of blockade where the number of electrons is fixed to N, to $(N+1)$, etc. Dashed and dotted lines describe steplike increases in the conductance and are explained in the text.

Fig. 3(b). The slopes of the boundaries are given by the ratio of the capacitances which can be calculated from Eq. (1). From Fig. 2(b) these ratios are obtained for peak 1: $C_r/C_G = 0.7$, $(C_l + C_G)/C_G = 1.9$. Consequently $\alpha = C_G/C$ is 0.4 ± 0.1, which agrees with the value obtained from the temperature dependence. From peak 1 to peak 4 the ratios increase. For peak 2 we have $C_r/C_G = 0.9$, $(C_l + C_G)/C_G = 2.3$. They are different because the geometrical capacitances depend on the spatial charge distribution.

In the regime of single-electron tunneling the conductance is increased for increased dc bias if during transport the dot can go either into the ground state or excited states of the $(N + 1)$ electron system. As the energy $\xi^*(N + 1)$ for an excited state is higher than the chemical potential $\xi(N + 1)$ the conductance is increased when $\xi^*(N + 1) + \Delta U(N + 1) \leq \mu_E$. This describes boundaries in the $V_G - V_{DS}$ plane [dashed lines in Fig. 3(b)] where an increase in conductance is caused by opening a new channel for tunneling at the emitter. At fixed V_{DS} the difference between current steps occuring at different gate voltages V_G and V_G^* is given by $V_G^* - V_G = (\alpha e)^{-1}[\xi^*(N + 1) - \xi(N + 1)]$.

Another channel is opened at the collector at sufficiently large dc bias V_{DS}, when the dot can stay either in an excited state or in the ground state of the N electron system after the $(N+1)$th electron has left the dot. The condition is $\xi(N+1) - \xi^*(N) + \xi(N) + \Delta U(N+1) \geq \mu_C$. Such boundaries are sketched in Fig. 3(b) as dotted lines. The distance between current steps reached for different gate voltages V_G and V_G^* at fixed dc bias is given by $V_G - V_G^* = (\alpha e)^{-1}[\xi^*(N) - \xi(N)]$.

The coupling of the different electronic states of the dot to the leads and the asymmetry of this coupling determine the observability of the current steps.[8] Comparing Fig. 2(b) with Fig. 3(b), one can see for peak 1 and positive V_{DS} at $B = 0$ T excited states of the N electron system are observed, whereas at $B = 1$ T an excited state of the $(N + 1)$ electron system is seen.

In Fig. 4(a) the magnetic-field dependence of the conductance σ versus V_G is shown. The magnetic field B is perpendicular to the 2D EG. For large B the amplitudes of all peaks are suppressed since the transmission through the barriers decreases with B. In accordance with this argument the intrinsic peak widths and cotunneling effects[1] decrease. So peaks become well separated with increasing B. In addition, there is simultaneous modulation of the peak amplitude and shift of peak position. The peak positions versus magnetic field B are plotted in Fig. 4(b). As in the case of the temperature dependence, peaks 1 and 2 and also peaks 3 and 4 show a similar behavior. This pairing of two peaks is understood in the one-particle picture of noninteracting electrons by the spin degeneracy of the energy states. So in the $\sigma(V_G)$ characteristics two peaks just separated by the Coulomb energy should appear.[3] The gate voltage differences between peaks 1 and 2 and peaks 3 and 4 are not the same. This may be explained by electron-electron interaction in the dot or changes in the capacitances caused by a rearrangement of the charge distribution in the dot and/or by the repulsion of the 2D EG in the leads for more negative gate voltages. As pointed out in the discussion of Fig. 2(b), the ratios of the capacitances differ from peak to peak.

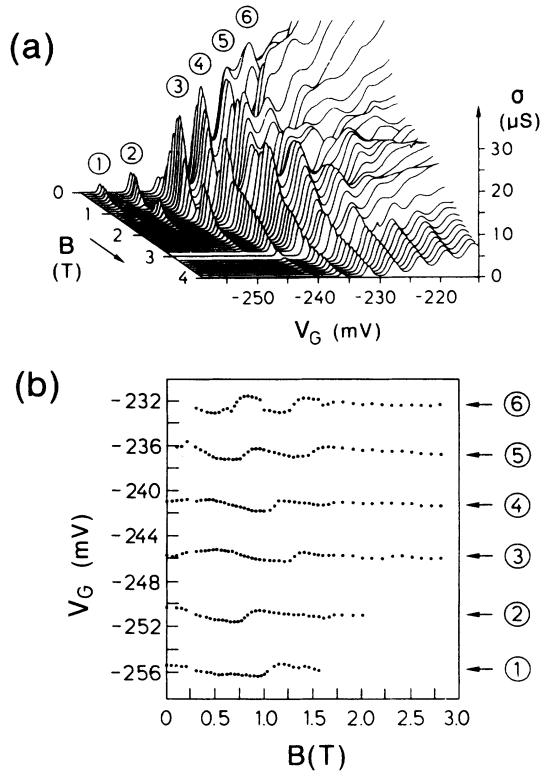

FIG. 4. (a) Conductance σ vs gate voltage V_G for magnetic fields $B = 0$ T to 4 T at $T = 730$ mK. The peak indices are given above. (b) V_G values of peak maxima vs magnetic field B. The peak indices are given to the right.

As expected from Eq. (1), changes in the chemical potential $\xi(N+1)$ with magnetic field move the position V_G of the conductance peak. For a qualitative understanding we compare our data with the one-particle energy levels versus magnetic field calculated by Fock[9] for a circular symmetric parabolic confinement and assume that the chemical potential $\xi(N+1)$ reflects the magnetic-field dependence of the one-particle energy E_{N+1} of the highest occupied one-particle state. At magnetic fields, where a crossing of eigenstates belonging to different Landau levels occurs, the character of the $(N+1)$th state is changed[5] affecting the amplitude and the position slope $\delta V_G/\delta B$ of the corresponding conductance peak. Peak 1 would correspond then to $(N + 1) = 7$, peak 6 to $(N + 1) = 12$. At low temperature even the slopes $[\delta V_G/\delta(\hbar\omega_C) = 1.6$ and $-0.9]$ obtained from our data for peak 2 at $B = 0.7$ T are consistent with Fock's calculation for the eighth state at the crossover of the eigenstate belonging to the first Landau level and the eigenstate belonging to the second Landau level. At this crossing the ratio between cyclotron energy $\hbar\omega_C$ and confinement energy $\hbar\omega_0$ is 0.76, from which an effective confinement energy 0.7 meV for our system is obtained (for peak 1 it is 1 meV).

In the one-particle picture it is expected that the transition between different Landau levels occurs at the same magnetic field for the two electrons occupying the same

spin-degenerate state (spin splitting for the bare g factor in GaAs is small). This is not in agreement with our data (see peak 1 and 2). McEuen *et al.*[5] observed the same deviation and have recently reinterpreted their data taking into account the Coulomb interaction in the dot.[10]

In conclusion, we have presented conductance measurements interpreted in the picture of single-electron tunneling through a quantum dot with few electrons under the tip of a gate finger. Differential conductance measurements in the $V_G - V_{DS}$ plane yield the ratio of the geometrical capacitances used in the model for a fixed number of electrons and are used as a tool for studying the spectroscopy of excited states.

We gratefully acknowledge stimulating discussions with R. Gerhardts, D. Heitmann, and H. Pothier. We thank M. Riek, J. Nieder, and F. Schartner for their expert help with the sample preparation. Part of the work has been supported by the Bundesministerium für Forschung und Technologie.

---

*Present address: Technische Universität Darmstadt, Petersenstrasse 20, W-6100 Darmstadt, Germany.

[1]Reviewed in Z. Phys. B **85** (1991) and in *Single-Electron Tunneling and Mesoscopic Devices*, edited by H. Koch and H. Lübbig, Springer Series in Electronics and Photonics Vol. 31 (Springer, Berlin, 1992).

[2]A. Groshev, Phys. Rev. B **42**, 5895 (1990).

[3]C.W.J. Beenakker, Phys. Rev. B **44**, 1646 (1991).

[4]L.P. Kouwenhoven, N.C. van der Vaart, A.T. Johnson, W. Kool, C.J.P.M. Harmans, J.G. Williamson, A.A.M. Staring, and C.T. Foxon, Z. Phys. B **85**, 367 (1991).

[5]P.L. McEuen, E.B. Foxman, U. Meirav, M.A. Kastner, Y. Meir, N.S. Wingreen, and S.J. Wind, Phys. Rev. Lett. **66**, 1926 (1991).

[6]T.E. Kopley, P.L. McEuen, and R.G. Wheeler, Phys. Rev. Lett. **61**, 1654 (1988).

[7]Y. Meir, N.S. Wingreen, and P.A. Lee, Phys. Rev. Lett. **66**, 3048 (1991).

[8]D.A. Averin, A.N. Korotkov, and K.K. Likharev, Phys. Rev. B **44**, 6199 (1991); A. Groshev, T. Ivanov, and V. Valtchinov, Phys. Rev. Lett. **66**, 1082 (1991); S.-R. Eric Yang and G.C. Aers (unpublished).

[9]V. Fock, Z. Phys. **47**, 446 (1928); e.g., Fig. 4 in Y. Hirayama and T. Saku, Solid State Commun. **73**, 113 (1990).

[10]P.L. McEuen, E.B. Foxman, J. Kinaret, U. Meirav, M.A. Kastner, N.S. Wingreen, and S.J. Wind, Phys. Rev. B **45**, 11 419 (1992).

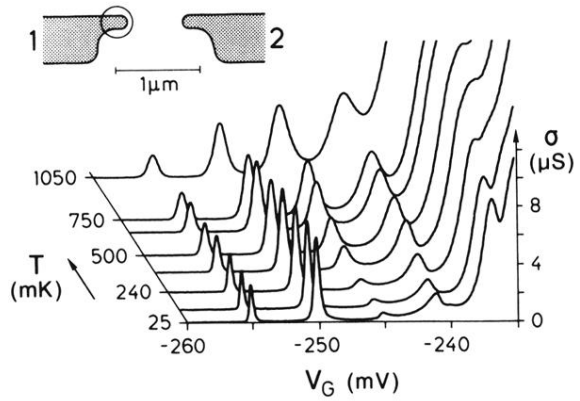

FIG. 1. Conductance σ vs gate voltage V_G for different temperatures T. Inset: Top view of the split-gate structure. The circle represents the region where we imagine the quantum dot.